#### Distribution Agreement

In presenting this thesis as a partial fulfillment of the requirements for an advanced degree from Emory University, I hereby grant to Emory University and its agents the non-exclusive license to archive, make accessible, and display my thesis in whole or in part in all forms of media, now or hereafter known, including display on the world wide web. I understand that I may select some access restrictions as part of the online submission of this thesis. I retain all ownership rights to the copyright of the thesis. I also retain the right to use in future works (such as articles or books) all or part of this thesis.

	July 17, 2025
Zachary Thacker	Date

# Investigating the Mechanics of Snake Climbing Through the Use of a Robot Analog By Zachary Thacker Master of Science Physics

Jennifer Rieser
Advisor

Justin Burton
Committee Member

James Kindt
Committee Member

Kurt Warncke
Committee Member

Accepted:

Kimberly Jacob Arriola, PhD, MPH
Dean of the James T. Laney School of Graduate Studies
July 17, 2025

Date

Investigating the Mechanics of Snake Climbing Through the Use of a Robot Analog

By

Zachary Thacker B.Sc., Berry College, 2023

Advisor: Jennifer Rieser

An abstract of
A thesis submitted to the Faculty of the
James T. Laney School of Graduate Studies of Emory University
in partial fulfillment of the requirements for the degree of
Master of Science
in Physics
2025

#### Abstract

Investigating the mechanics of snake climbing through the use of a robot analog

#### By Gauge Thacker

Snakes provide an excellent example of limbless locomotion in nature. Animal movement is often highly variable and difficult to fully reproduce as animals are often influenced by a wide array of outside factors, and snakes are no exception. This can cause potential inconsistency in measurements taken of the movement of real snakes, which can make research into snake movement more difficult. While there have been previous attempts to understand how snakes climb through the use of coiling their bodies, there is limited research that seeks to understand snake climbing that relies on the snake weaving its body between obstacles, a form of movement that snakes engage in to climb between gaps in tree bark. In order to analyze the interactions occurring during snake climbing in a more controlled and consistent manner, we built a robot snake that serves as a simple model for serpentine motion with the ability to change several movement parameters. We then tuned these parameters to produce a wave of bending along the snake's body that matches the geometry of a board of regularly spaced pegs. Our snake robot was able to successfully climb a vertical peg wall with pegs evenly spaced 10.2 cm, 12.7 cm, and 15.2 cm apart, and was able to do so both upwards and downwards. We believe that this identifies a minimal condition for climbing, and suggests that reliance on friction is not necessary for this climbing method.

Investigating the Mechanics of Snake Climbing Through the Use of a Robot Analog

By

Zachary Thacker B.Sc., Berry College, 2023

Advisor: Jennifer Rieser

A thesis submitted to the Faculty of the Emory College of Arts and Sciences of Emory University in partial fulfillment of the requirements for the degree of Master of Science in Physics 2025

#### Acknowledgements

Dr. Jennifer Rieser has been invaluable to my academic experience over the last two years. The knowledge and guidance she provided me with has been crucial to my ability to make it this far in my academic career. I am also grateful to Dr. Burton, Dr. Warncke, and Dr. Kindt for being members of my thesis committee.

I would not be where I am today without the love and support given to me by Morgan Anderson, who has been both a wonderful partner and an amazing influence on my life in general. Without her I would be compltely lost in this world.

I am proud to consider Drisha Sehgal, Alex Vargas, Michelle Wang, and Zach Germain as both coworkers and friends, and could not imagine making it this far without their continual support.

I would also like to thank Shiloh and Charlotte, who were both wonderful friends during what little time we had together.

Finally, I would like to thank my mother, who has supported me throughout this entire process and more.

## Contents

1	Intr	roduction	1
	1.1	Methods of Snake Locomotion	3
		1.1.1 Sidewinding and Rectilinear Locomotion	3
		1.1.2 Concertina	£ 5
		1.1.3 Lateral Undulation	8
	1.2	Previous Work in Robotics	10
		1.2.1 Intricate Robotics	10
		1.2.2 Simple Robotics	13
	1.3	Motivation	14
	1.4	Thesis Outline	15
2	Exp	perimental Design	17

	2.1	Snake Design	17
	2.2	Pegboard Design	25
	2.3	Climbing Trials	28
3	Res	ults	30
	3.1	Trajectories	30
	3.2	Angle Between Segments	33
	3.3	Wavelength	37
	3.4	Displacement Per Cycle	38
4	Disc	cussion	41
	4.1	Climbing Success	41
	4.2	Trajectories	42
	4.3	Angle Between Segments	43
	4.4	Displacement Per Cycle	44
	4.5	Peg Spacing Limitations	47
5	Con	nclusion	52
	5.1	Future Work	53
	5.2	Applications	56

# List of Figures

1.1	Dorsal view of sidewinding movement. Adapted from Ref [16]	4
1.2	Snake undergoing concertina locomotion on flat horizontal surface. Taken	
	from Jayne, Integrative and Comparative Biology (2020) [13]	7
1.3	Top and side view of lateral undulation on a cylinder. Taken from Jayne,	
	Integrative and Comparative Biology (2020) [13]	S
1.4	A) Snake robot that uses preset movements, such as algorithms which allow	
	for pole climbing, forward movement, etc., in conjunction with manual control	
	of snake's head to move [26]. B) Climbing robot that uses claw-like feet and	
	a flexible body to climb cylindrical objects [27]. C) Snake robot that uses	
	movement in multiple axes to create loops in its body to climb ladders [28]	12

2.1	A) Splined recreation of captured data from force-sensitive pegboard climbing	
	experiments of a live snake. The snake is observed to follow an approximately	
	serpenoid movement pattern along its body. Head is at the top of the body	
	show, while tail is at the bottom. Red dots represent pegs. Arrows represent	
	the force applied on pegs by snake. Black sections of snake's body represent	
	body segments that are removed from other analysis to provide more reliable	
	results. B) Spacetime plot of same live snake trial, where $\kappa\lambda$ is the curvature	
	of the snake normalized by the average length of a wave on the body. Credit:	
	Calivn Riiska	19
2.2	Motor assembly of the robot snake. Fifteen motors were used in the total	
	construction	20
2.3	Diagram of obtaining $\theta$ from two motors. $\vec{V}_i$ is a vector of arbitrary length	
	that lies along the body of motor $i$ . $\phi_i$ and $\phi_{i+1}$ are the angles $\vec{V}_i$ and $\vec{V}_{i+1}$	
	make with the bottom of motor $i$ respectively	22
2.4	Woven plastic skin used to prevent wires becoming tangled on pegs. Silver	
	circles on skin are marker stickers used to track snake movement	24

2.5	Pegboard in the 15.2 cm configuration. Aluminum T-frame behind poster-	
	board covering allows for pegs to be slid to desired positions and held in place	
	with screws. Poster-board cover prevents snake from getting caught behind	
	pegs	27
3.1	A) Example trajectory plot for the 10.2 cm peg spacing, upwards movement.	
	B) Example trajectory plot for the 12.7 cm peg spacing, upwards movement.	
	C) Example trajectory plot for the 15.2 cm peg spacing, upwards movement.	
	Due to height constraints on the pegboard, the lowest peg on the 15.2 cm	
	trials was too close to the ground to be used and has been omitted from the	
	results for this spacing. D) Example of robot snake's body not following the	
	position of the head on previous timesteps. Red points represent locations of	
	the head that the snake's body never visits	31
3.2	Trajectory plots for the 12.7 cm peg spacing. Movement is upwards and	
	downwards respectively. Each plot is created from one trial, and serves as an	
	example for the movement seen in each movement direction	32
3.3	Theoretical angle between motors of a serpenoid curve corresponding to the	
	12.7 cm peg spacing moving upwards with respect to time	35

3.4	A) Measured angles between motors of a serpenoid curve corresponding to the	
	12.7 cm peg spacing moving upwards with respect to time. B) Horizontal line	
	between two points in time in which a given segment has the gone through a	
	full cycle, used to measure period. C) Vertical line between two segments with	
	equal angles, used to measure wavelength. D) Robot snake tracking data of	
	two different time points two cycles apart. Black points represent end of body	
	segments that do not have an angle associated with them. $\lambda$ is wavelength.	
	E) A point on the robot snake's body. F) The same point two cycles later	36
3.5	Wavelength of motion for each peg spacing, up and down. Error bars represent	
	one standard deviation for the ten trials used to find the wavelength for a given	
	set of parameters	37
3.6	Average displacement per cycle for each peg spacing, up and down. Error bars	
	represent one standard deviation for the ten trials used to find the average	
	displacement per cycle for a given set of parameters	40

4.1	Example of robot shape that works while the robot snake is traveling upwards,	
	but would not be possible while the robot snake is traveling downwards, re-	
	sulting in the need for a slightly different set of parameters for upwards and	
	downwards motion. Red circles represent pegs, and red areas on motors rep-	
	resent areas the motor could not physically occupy. Black arrows represent	
	direction of travel	46
4.2	Theoretical peg spacing that would be impossible to navigate based on the	
	physical constraints of the robot snake's body. Red circles represent pegs, and	
	red areas on motors represent areas the motor could not physically occupy	49
4.3	Interpolated tracking data from 17.8 cm peg spacing trial. Robot snake main-	
	tains only two points of contact at some points while climbing	51
5.1	New tracking system being tested on robot snake	54

## List of Tables

2.1	Robot Snake Movement Parameters.				 							2	5

## Chapter 1

## Introduction

The world around us provides a diverse collection of environments, each with their own plethora of living beings adapted to the unique conditions they live in. This has resulted in a wide variety of locomotion methods among living beings, such as birds that fly overhead, fish that swim under the waves, and people that walk by alternately moving two points of contact with the ground. Despite the diversity seen among these locomotion methods, there is still often one major similarity: the use of appendages.

Birds have wings, fish have fins, humans have legs, but not all animals use appendages to move through the world. Snakes stand out as a common but diverse example of movement without the use of appendages, instead relying only on their body's ability to push off of surfaces, which has been studied for over seventy years [1, 2], in conjunction with subtle movements of their scales, which is a more recent area of study [3]. Research that focuses on understanding the mechanics of snake movement is diverse and extensive [4, 5, 6, 7, 8, 9, 10], however, existing literature often focuses on understanding the relationship between snake movement and internal structures within the snake's body, such as the snake's muscles and bones. As a result, research into the relationship between snake movement and the forces applied by the snake to the world around them is less robust in comparison, which has created a gap that we hope to begin to fill.

Throughout the course of this thesis we focused on three major points of interest:

- 1. We investigated the ability of snakes to climb surface protrusions by matching their bodies to surface geometry.
- 2. We determined the importance of friction for this method of snake climbing.
- 3. We created a physical model of snake movement that produces consistent results under set parameters.

#### 1.1 Methods of Snake Locomotion

Current research into snake locomotion largely involves consideration of four main types of movement: sidewinding, rectilinear locomotion, concertina, and lateral undulation. The form of movement a snake chooses to use is sometimes dependent on the environment the snake is moving in or the species of snake among other factors [11, 12], and the underlying mechanics involved with each type of movement can vary substantially.

#### 1.1.1 Sidewinding and Rectilinear Locomotion

Sidewinding movement displays the following characteristics: parts of the snake's body maintain static contact with the ground during movement, every point along the snake follows a path that is distinct but roughly parallel to all other points, and the creation of disconnected parallel tracks that are oblique to the direction of movement due to the areas of the snake undergoing nearly static contact [13], which are the orange areas seen in Fig 1.1. Sidewinding is seen most often as a form of movement across surfaces made of granular media, such as sandy deserts [14, 15], though it is not limited to these areas, also being seen in other areas, including hardpan deserts [14, 16]. Since sidewinding is typically only used for traversing large, uncluttered surfaces, my work will not include any attempt to replicate this motion,

as it is unimportant to climbing.

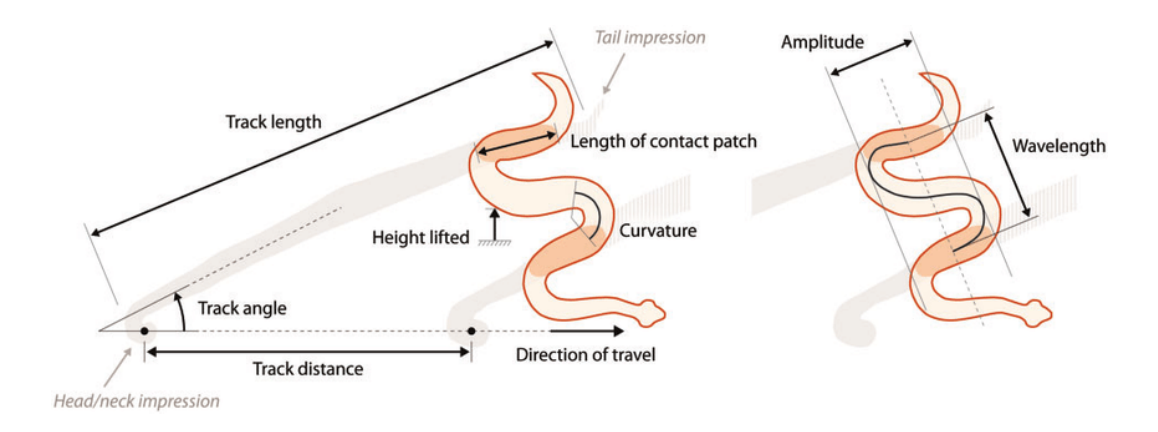


Figure 1.1: Dorsal view of sidewinding movement. Adapted from Ref [16].

Rectilinear locomotion differs from all other forms of snake locomotion as it relies on anatomical structures not utilized in any other form of locomotion [13]. Unlike the other forms of locomotion that rely on pressing parts of the body against a surface to generate force, rectilinear locomotion relies on using muscles attached to the ribs of the snake that either rotate or stabilize the ribs to allow the skin of the snake to move over the ground, pulling the snake forwards, though there is still some uncertainty in the exact mechanics of this process [17]. This form of locomotion is also unique as it allows the snake to move while its body remains straight, with all other forms of locomotion requiring bends in the snake's body. While rectilinear locomotion could theoretically be used during snake climbing,

as other groups have utilized rectilinear locomotion with a robot snake analog to climb a surface at 4° elevation [18], to our knowledge use of this form of locomotion by live snakes for climbing has yet to be described in literature. Therefore, I will not replicate this form of locomotion in my work, and instead focus on more common types of climbing locomotion.

#### 1.1.2 Concertina

Concertina locomotion involves a snake creating static anchor points with a surface and using these anchor points to move other parts of its body forward, at which point the snake will choose new regions of its body to use for static contact and repeat the process. Concertina locomotion can be used on horizontal surfaces, cylinders, and in tunnels [13], and is highly reliant on frictional effects in order to be successful [19]. Unlike both sidewinding and lateral undulation, concertina movement does not rely on propagating repeating bends along the snake's body, instead relying on anchor points that allow for the snake's body to stretch forward, which does not always demonstrate repetition. An example of a snake undergoing concertina locomotion can be seen in Fig 1.2. Concertina locomotion can be substantially more complicated than the other forms of snake locomotion, requiring active decision making to decide what parts of the body should remain in static contact with the ground at any given moment. While concertina locomotion is present in snake climbing [20], and previous

experiments conducted in Rieser lab have observed snakes climbing pegs through the use of concertina motion alongside lateral undulation, concertina motion is more complicated, and as such our research is currently focused on live snakes climbing through the use of lateral undulation, which is explained in more detail in Section 1.1.3.

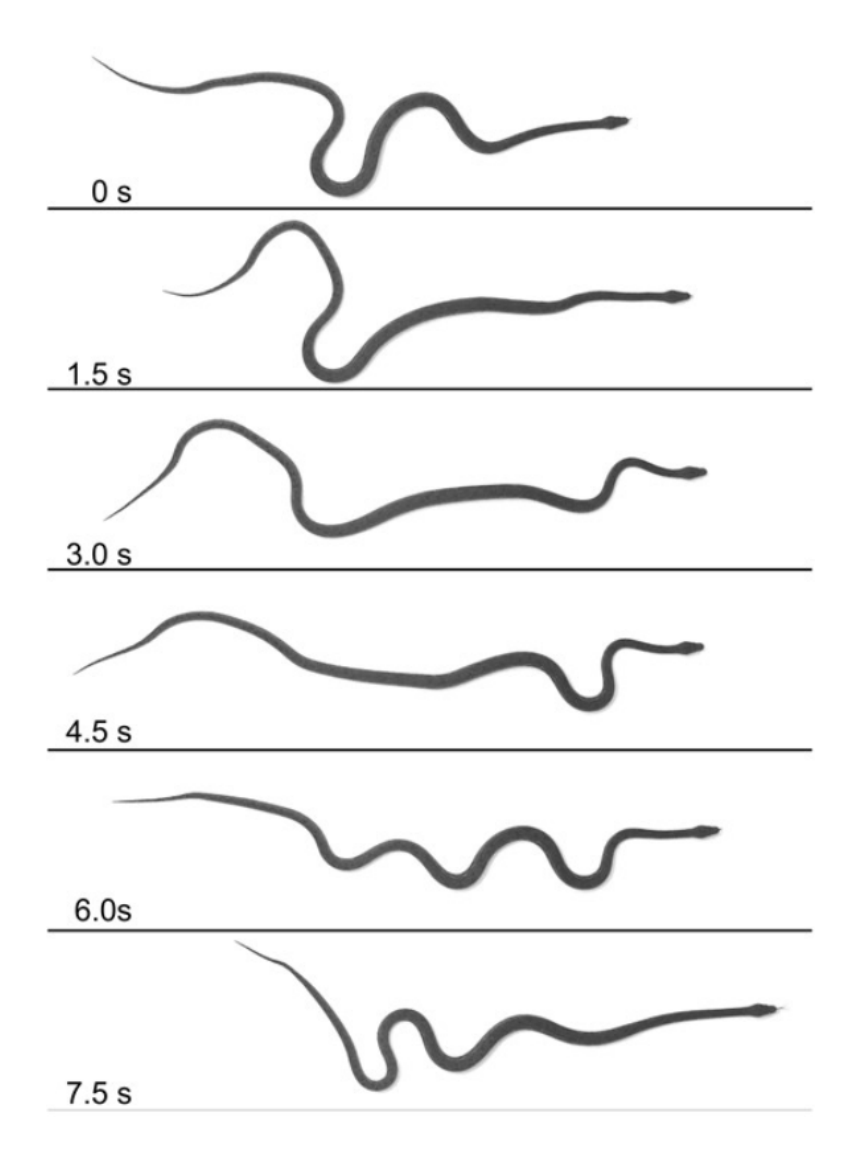


Figure 1.2: Snake undergoing concertina locomotion on flat horizontal surface. Taken from Jayne, Integrative and Comparative Biology (2020) [13]

#### 1.1.3 Lateral Undulation

Lateral undulation, also referred to as serpentine motion, involves the propagation from head to tail of waves of lateral bending along an animal's body to propel the organism forward [21]. This form of locomotion is useful for both terrestrial movement as well as aquatic movement, although aquatic lateral undulation typically involves the propagation of a wave that increases in both amplitude and wavelength over time, while terrestrial lateral undulation more often relies on waves that maintain a consistent wavelength and amplitude [13]. Terrestrial lateral undulation is also unlike aquatic lateral undulation as during this form of locomotion snakes can rely on objects in their environment to prevent slippage, such as the branches of a tree. Both concertina and lateral undulation can be used to navigate arboreal environments, as both allow for the snake to rely on objects in their environment to propel themselves forwards. An illustration of lateral undulation can be seen in Fig 1.3.

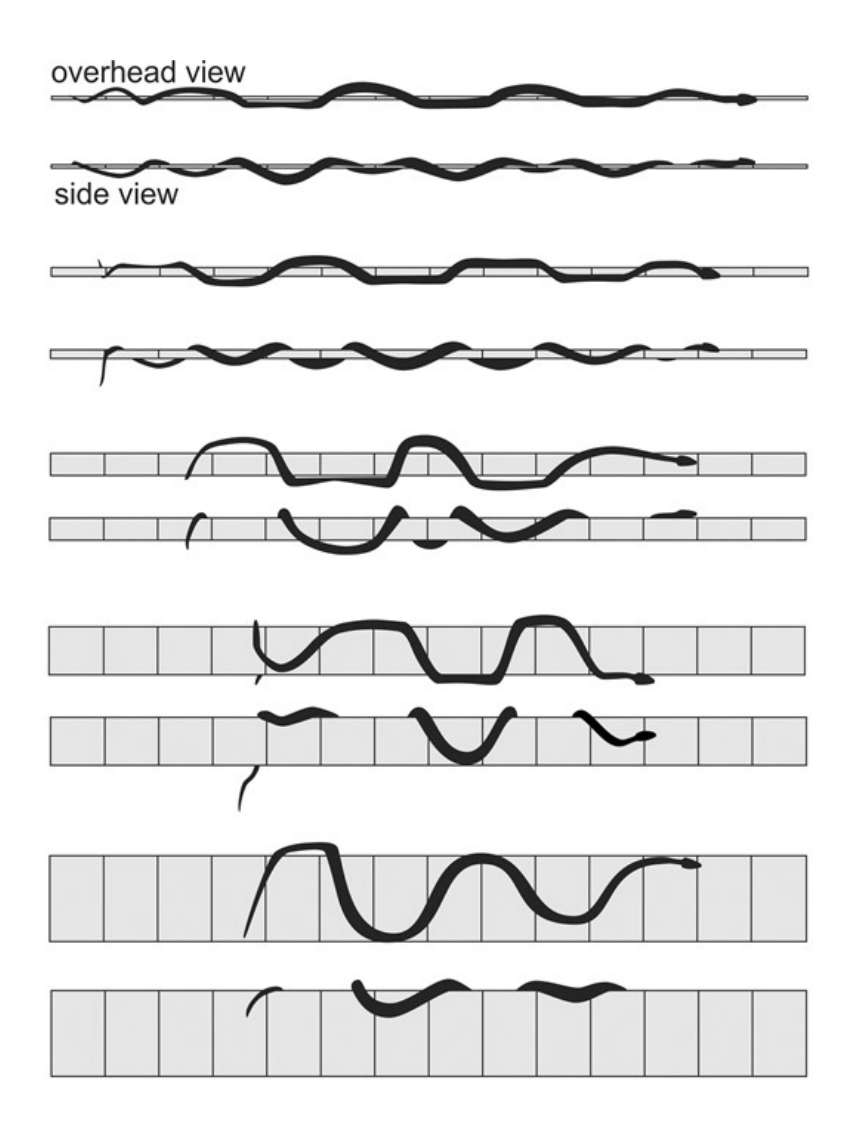


Figure 1.3: Top and side view of lateral undulation on a cylinder. Taken from Jayne,

Integrative and Comparative Biology (2020) [13]

#### 1.2 Previous Work in Robotics

#### 1.2.1 Intricate Robotics

Multiple successful attempts have been made at producing robots that can navigate surfaces in a snake-like manner. Examples of these can be seen in Fig 1.4. These robots commonly use intricate gripping mechanisms in order to grab onto objects or surfaces, or utilize both pitch and yaw rotation in order to achieve movement outside of a single plane. These more complex robot designs allow for a wide range of movement and more adaptability to irregular terrain, but also adds complexity to the designs, such as requiring multiple unique moving parts or a more elaborate control algorithm, and can introduce multiple points of failure as new components are added and increase costs [22]. Due to the downsides of complex robots, it is useful to create simplified robots that model the desired form of movement, as this reduces the presence of uncontrollable complexities that occur when using more intricate designs [23, 24].

Examples of more complicated robots that mimic climbing behavior similar to what is seen in snakes include the U-Snake, which uses up to 36 motorized joint modules that are 90° offset from each other in order to achieve three dimensional shapes [25]. U-Snake uses a head

mounted camera and LED system to provide video feedback of its surroundings, and uses a gamepad to modify movement parameters such as speed and amplitude or to switch between preset poses, and combinations of these controls can be used to swap between behavioral patterns, such as sidewinding, pole climbing, or independent head control [26]. Another example of a more complicated climbing robot is Treebot, which utilizes two omnidirectional grippers connected to the ends of a continuum manipulator to alter the position of the grippers relative to each other, allowing for one gripper to remain stationary as the other gripper is repositioned in order to move Treebot to a new location [27]. Another example of a climbing robot is the ladder climbing robot created by Tatsuya Takemori et al. [28]. This robot is similar to U-Snake in that it is created by chaining together motors that are 90° offset from each other in order to achieve three dimensional movement, however, this robot utilizes a novel gait design that combines straight and helically coiled segments in order to form hanging loops over the rungs of a ladder in order to climb.

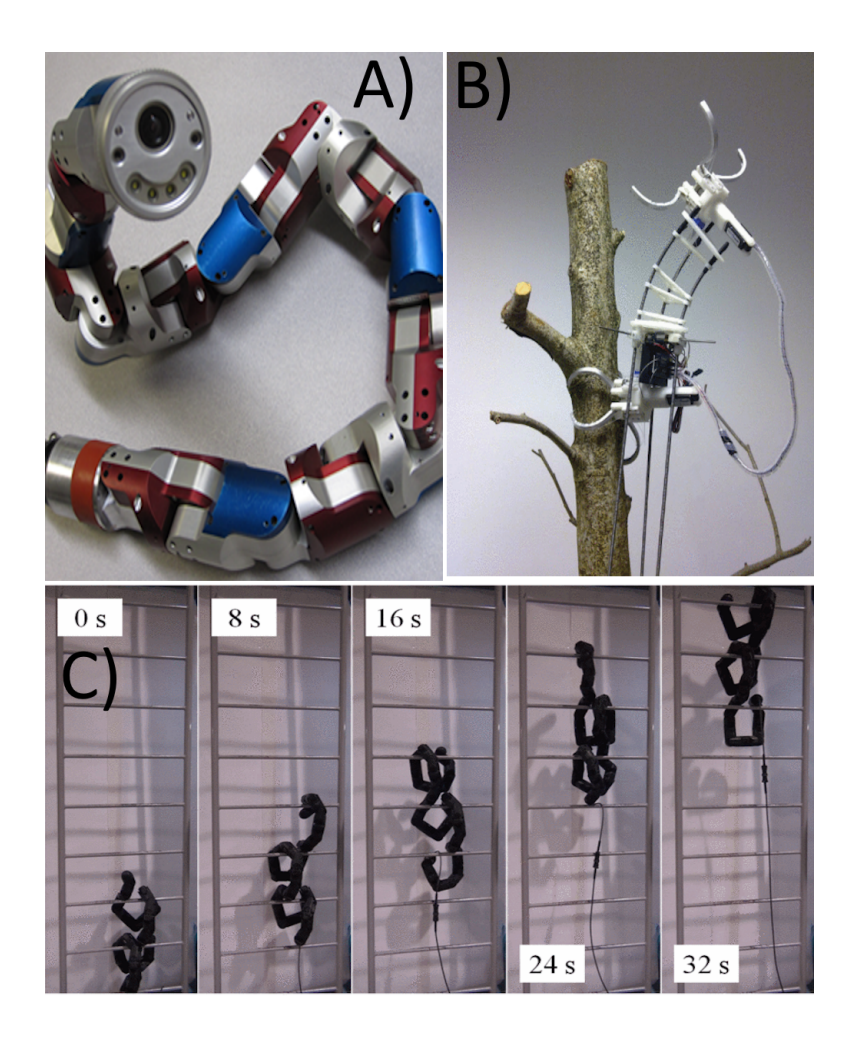


Figure 1.4: A) Snake robot that uses preset movements, such as algorithms which allow for pole climbing, forward movement, etc., in conjunction with manual control of snake's head to move [26]. B) Climbing robot that uses claw-like feet and a flexible body to climb cylindrical objects [27]. C) Snake robot that uses movement in multiple axes to create loops in its body to climb ladders [28].

#### 1.2.2 Simple Robotics

Less complex robots are still able to perform several useful tasks and are often easier to model and understand. While other groups have developed snake robots that rely on alternating pitch and yaw motors that require human oversight to move effectively [26, 28], or complicated feedback systems to provide updates on the position of the snake's body [29], these robots are still difficult to model and analyze, promoting the creation of a simplified robot that still uses this body plan. An example of this body plan being simplified can be seen in the robot constructed by Qiyuan Fu et al. [30], which achieves movement by sending a single sinusoidal wave through a chain of motorized body segments that are rotated 90° from each other in conjunction with one way wheels on each body segment to both move forwards and climb ledges. Scalybot serves as an example of another simple robot meant to mimic a form of snake locomotion, as it uses a simple two-part body that can control the distance between its two body segments, along with the ability to control how much friction is present between these body segments and the floor, to move in a manner that resembles a mixture of rectilinear and concertina locomotion [31]. One of the earliest snake robots to mimic serpenoid motion was created by Shigeo Hirose, and utilized linked servos to create bending motion in a single plane similar to our own snake robot [32]. The reduced complexity of these models often lowers the costs to produce them and limits sources of failure.

While previous research has produced snake robots that can climb up ledges [30], inclined surfaces [31], and poles [26], there has been little investigation into recreating the ability of arboreal snakes to weave between tree branches or tree bark asperities to climb vertical surfaces. In order to understand how real snakes can climb trees by weaving between branches or asperities, we wanted to compare the movement seen in real snakes to a controllable analog that can be studied more easily. However, we were unable to find a deep investigation of robot analogs that climb in this manner, motivating the creation of our robot snake in order to study this gap in existing literature.

#### 1.3 Motivation

Another member of Rieser lab, Calvin Riiska, has conducted several experiments using a motion tracking camera system and force sensitive pegboard to track and analyze the movement of live snakes as they climb up and down the pegboard. These experiments provide useful information for understanding the relationship between snake movement and the environment around them when successful, and prompted us to investigate if snakes can climb

between pegs by simply matching their movement to the geometry of the pegboard. This inspired us to investigate the ability of snakes to climb between pegs by only matching the bodies to the geometry of the pegs they are climbing. To test this, we created our robot snake and tasked it with climbing between pegs on a pegboard. Due to our robot snake being successfully able to climb the pegboard, we were inspired to create a computational model of snake climbing. Calvin has begun working on a computational model of snake movement, which will be compared to the results obtained using our robot snake in order to verify the accuracy of the model to real world snake climbing.

#### 1.4 Thesis Outline

Contained within this thesis are 5 sections that outline the efforts undertaken to characterize and understand the movement of our robot snake in pursuit of a Master of Science degree at Emory University.

Section 2 explains the experimental design of the robot snake and the manner in which trials were conducted to collect data from our robot snake.

Section 3 details the data collected from the robot snake, how it was processed, and general trends seen within the data.

Section 4 details the information we have learned through the analysis of these results.

Section 5 is the conclusion, future directions, and applications of this work.

## Chapter 2

## Experimental Design

#### 2.1 Snake Design

While the use of live snakes to study snake movement provides valuable insight into the ways in which real snakes move, live snakes can be difficult due to the highly variable behavior of the snakes. Robots, on the other hand, provide a reliable and programmable platform through which we can systematically vary control parameters and test hypotheses, while retaining the guarantee that their movement is physically possible, which is not always easy to achieve using simulations. Despite the difficulty often involved in creating computation models of real world movement, these models are still useful, though these models should be

verified using real world experiments to ensure accuracy. In order to better understand the behaviors seen in our experiments using real snakes, we created a robot snake that mimics snake movement by following a serpenoid curve that is observed in live snakes, which can be seen in Fig 2.1. Due to the success of our robot snake, we were inspired to create a computational model of snake movement that will be validated through comparison to the data collected from experiments using our robot snake. In order to model lateral undulation we constructed a robot snake similar to previous robots used to model undulatory movement in snakes [32]. The robot snake used in our experiments consists of fifteen Dynamixel XC330-T288-T motors that are attached to each other using 3D resin printed brackets. All brackets maintain the same orientation relative to their corresponding motor for all motors along the snake's body, resulting in a snake whose body can only experience bending within a plane shared by all motors. A photograph of this design can be seen in Fig 2.2.

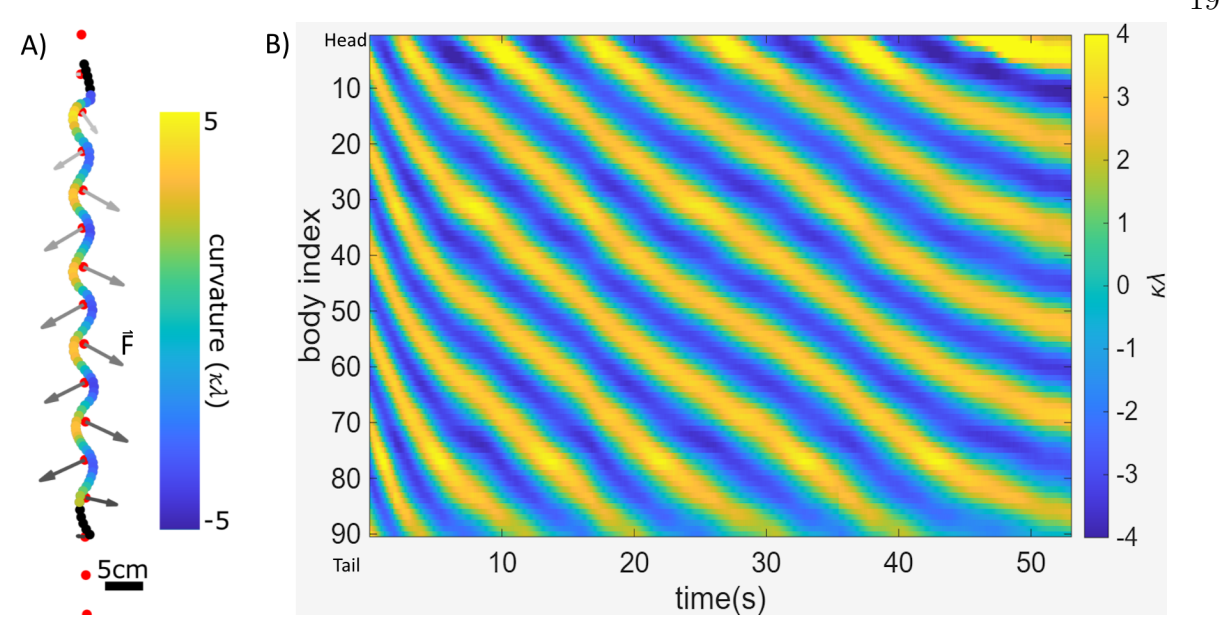


Figure 2.1: A) Splined recreation of captured data from force-sensitive pegboard climbing experiments of a live snake. The snake is observed to follow an approximately serpenoid movement pattern along its body. Head is at the top of the body show, while tail is at the bottom. Red dots represent pegs. Arrows represent the force applied on pegs by snake. Black sections of snake's body represent body segments that are removed from other analysis to provide more reliable results. B) Spacetime plot of same live snake trial, where  $\kappa\lambda$  is the curvature of the snake normalized by the average length of a wave on the body. Credit: Calivn Riiska.

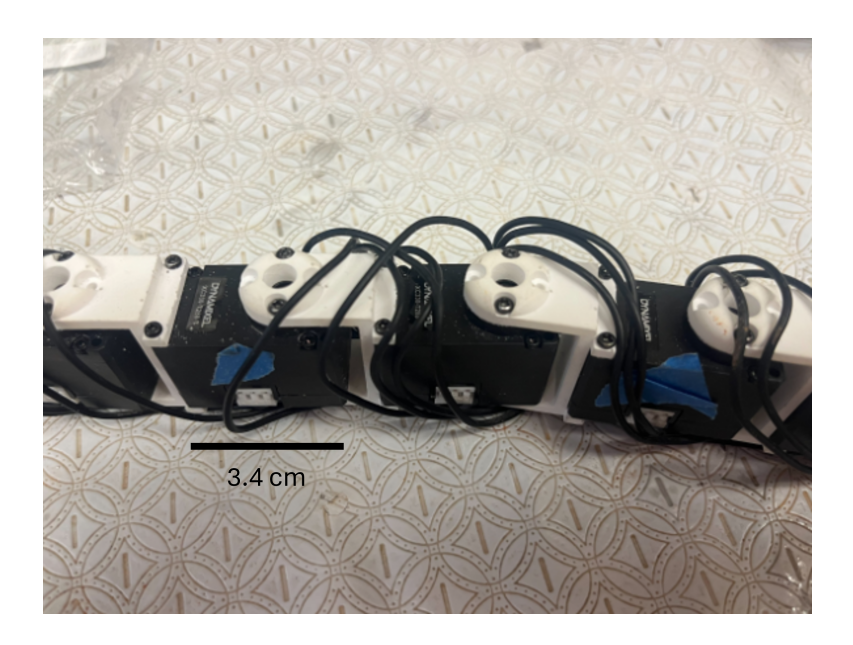


Figure 2.2: Motor assembly of the robot snake. Fifteen motors were used in the total construction.

The motion of our snake robot was controlled through the use of target angles that were given to each motor. The motors were given instructions through the use of an Arduino Uno and a Robotis U2D2 USB communication converter. In order to produce a serpenoid curve along the robot snake's body, each motor followed target angles,  $\theta$  given by the equation:

$$\theta_i(t) = B_0 \xi \sin(2\pi \xi \frac{i}{N} + 2\pi f t), \qquad (2.1)$$

where N=15 is the number of motors that comprise the snake robot, i is the index of the motor to which the goal angle is being assigned,  $\xi$  is the number of waves on the snake's body,  $B_0$  is the angular amplitude in radians, and  $f=10\frac{1}{dt\cdot N}$  is the frequency of the motion of the snake's body, where dt is the time between sent motor commands, and the factor of 10 is introduced to set the speed of the robot snake's movement within a range that is both fast enough to result in trials that take less than a minute without moving so fast that the resulting stress on the snake's body breaks the brackets that connect the motors. A diagram of how  $\theta$  relates to two motors can be seen in Fig 2.3

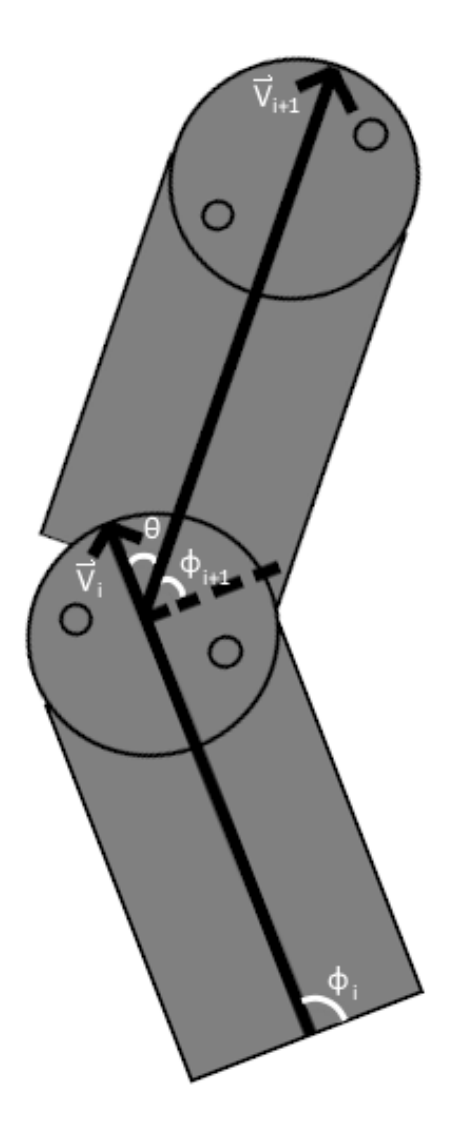


Figure 2.3: Diagram of obtaining  $\theta$  from two motors.  $\vec{V}_i$  is a vector of arbitrary length that lies along the body of motor i.  $\phi_i$  and  $\phi_{i+1}$  are the angles  $\vec{V}_i$  and  $\vec{V}_{i+1}$  make with the bottom of motor i respectively.

The python script used to control the motion of our robot snake uses a fixed number of steps within a given cycle of motion. Therefore, in order to cover a larger range of  $\theta(t)$  within a cycle, the amount of angle covered between each motor command must increase. This results in jerky motion when the range that  $\theta(t)$  covers per cycle is large. This resulted in the need to modify dt to allow for certain parameter sets. An alternative to this would be to maintain a fixed value of the angle covered between motor commands, allowing for a consistent value of dt between all trials, but requiring more motor commands per cycle for larger angular amplitudes.

The snake's body was placed within a flexible woven plastic skin, which can be seen in Fig 2.4, to reduce the chance of exposed wires becoming caught on the pegboard. We placed 15 reflective circular markers onto the snake's skin, with one being placed over the rotation point of each motor when the snake was at rest and fully straight. The snake's motion was recorded with six Optitrack Prime<sup>x</sup> 22 cameras in order to prevent markers from being completely obscured by pegs as the snake robot weaved around them. Video was captured at 60 frames per second and markers were automatically isolated by the camera's integrated image processing. This data was then used to track the robot snake's movement in 3-D for further analysis.

The movement parameters for each peg spacing can be seen in Table 2.1.



Figure 2.4: Woven plastic skin used to prevent wires becoming tangled on pegs. Silver circles on skin are marker stickers used to track snake movement.

Table 2.1: Robot Snake Movement Parameters.

Peg Spacing (cm)	10.2	10.2	12.7	12.7	15.2	15.2
Climb Direction	up	down	up	down	up	down
dt (s)	.024	.024	.016	.016	.016	.016
$B_0$ (radians)	.47	.47	.5	.5	.5	.5
$\xi$	2.3	2.4	2.0	2.15	1.65	1.8

The parameters listed in Table 2.1 were not theoretically derived, and were instead determined by testing different combinations of parameters until the crests in the robot snake's body were spaced the same distance apart as the pegs in the pegboard setup we were attempting to match the geometry of, and the angular amplitude was set so that the robot snake could effectively move between pegs without damaging itself.

#### 2.2 Pegboard Design

The pegboard the robot snake has been tasked with climbing consists of 8 horizontal PVC pipes that are 2.1 cm in radius spaced equal distances apart vertically. The coefficient of static friction between the robot snake's skin and a PVC peg is measured as  $\mu = 0.255\pm0.006$ . The coefficient of static friction is measured by placing the skin of the robot snake on a flat

surface, placing the PVC pipe onto the skin so that it will slide down the skin instead of rolling, and tilting the flat surface until the PVC pipe begins to slide down the skin's surface at an approximately constant speed. From here, the angle of the flat surface is found by measuring the horizontal and vertical distance between its two ends and taking the inverse tangent of the horizontal distance between the two ends of the surface divided by the vertical distance between the two ends of the surface. This measurement was repeated ten times. This results in relatively low friction in our system, which is present at points where the robot snake's body contacts a pipe. These spacings were: 10.2 cm, 12.7 cm, and 15.2 cm for the trials conducted as part of this experiment. Our setup involves screwing the PVC pipes onto a bracket held by T-Slot aluminum railing, which allows the pipes to be positioned at any spacing that does not result in two pipes intersecting each other or a pipe intersecting with a support beam. This setup allows for pegs to be spaced at any distance from each other that does not result in distance between the first and last peg exceeding the height of the pegboard. This setup also allows for pegs to be spaced at irregular intervals, however, none of our experiments utilized this feature. A photograph of this setup can be seen in Fig 2.5.



Figure 2.5: Pegboard in the 15.2 cm configuration. Aluminum T-frame behind poster-board covering allows for pegs to be slid to desired positions and held in place with screws. Poster-board cover prevents snake from getting caught behind pegs.

#### 2.3 Climbing Trials

Ten trials were conducted for each combination of movement direction and peg spacing, resulting in sixty trials in total. Each trial began by beginning to record the motion of the snake in OptiTrack. We then initialized the python script (Credit: Jennifer Rieser, Zach Germain, Rory Flint) responsible for sending target angle data to each motor to form the serpenoid curve given by Eq 1, which provides an adjustable delay period in which the snake assumes the waveform given by Eq 1 with t=0 without advancing t. During this delay period, the snake is placed on the wall so that it does not fall off, usually requiring a minimum of three points of contact between the snake's body and the pegboard. After the delay period ends, the snake begins to climb the wall using the serpenoid equation with the provided parameters for a given combination of movement direction and peg spacing. Once the snake had successfully climbed to the other end of the pegboard and was either in danger of falling off or hitting the floor, the script controlling the robot snake was terminated and the snake was removed from the pegboard, at which point the OptiTrack recording was ended. During trials involving downward movement, the wire that provides power and control to the snake's motors needed to be held away from the pegboard so that it did not bind on the pegs and alter the snake's motion. This was done by manually holding the wire so that it was always slack, minimizing the force applied to the snake by the power and control wires.

# Chapter 3

# Results

### 3.1 Trajectories

Trajectory plots were made for trials from each peg spacing, the results of which can be seen in Fig 3.1 and 3.2. The trajectory plots were made by creating a 100 point spline at each timestep and plotting the resulting spline with a time dependent color. Splines were created using a modified Akima interpolation method in MATLAB. This interpolation method performs cubic interpolation to create piecewise polynomials that have continuous first-order derivatives [33].

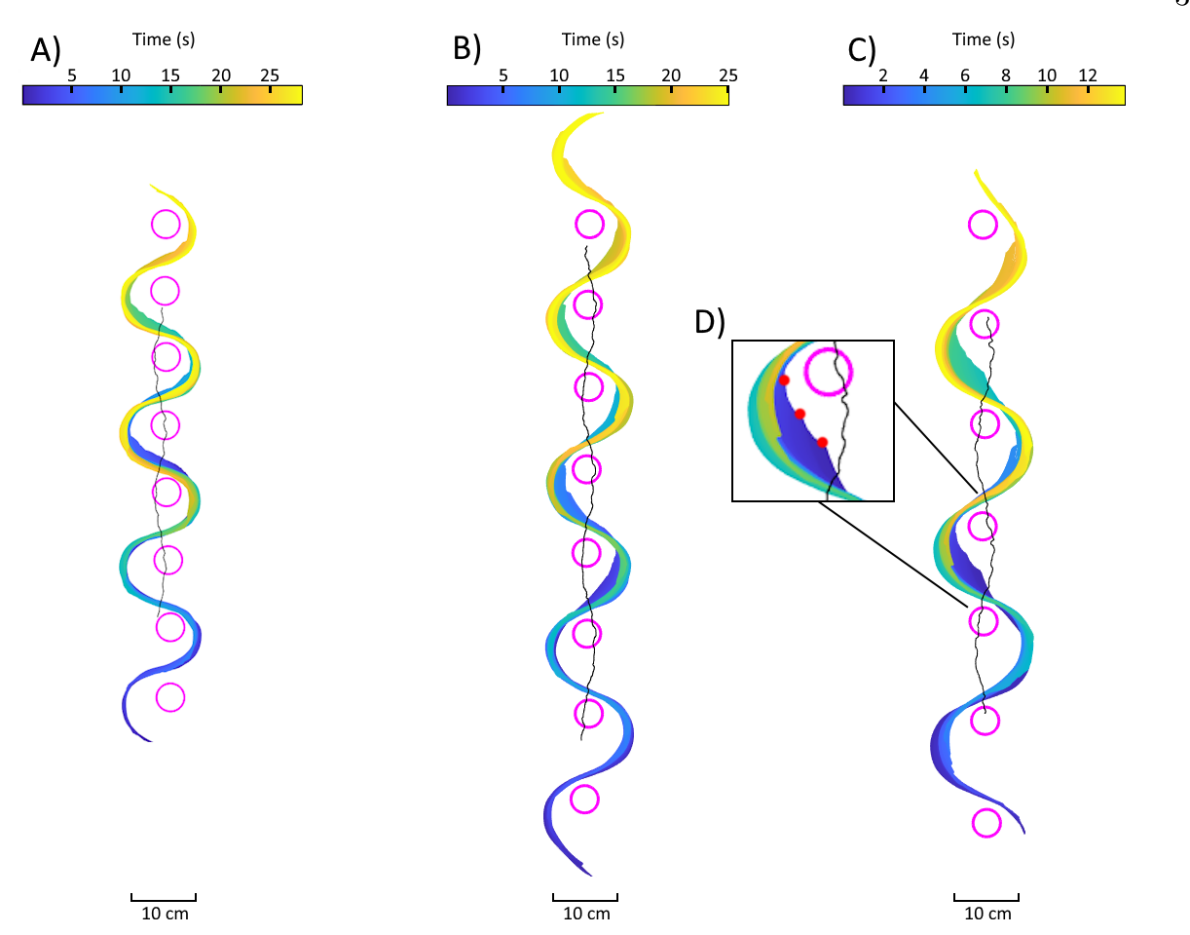


Figure 3.1: A) Example trajectory plot for the 10.2 cm peg spacing, upwards movement. B) Example trajectory plot for the 12.7 cm peg spacing, upwards movement. C) Example trajectory plot for the 15.2 cm peg spacing, upwards movement. Due to height constraints on the pegboard, the lowest peg on the 15.2 cm trials was too close to the ground to be used and has been omitted from the results for this spacing. D) Example of robot snake's body not following the position of the head on previous timesteps. Red points represent locations of the head that the snake's body never visits.

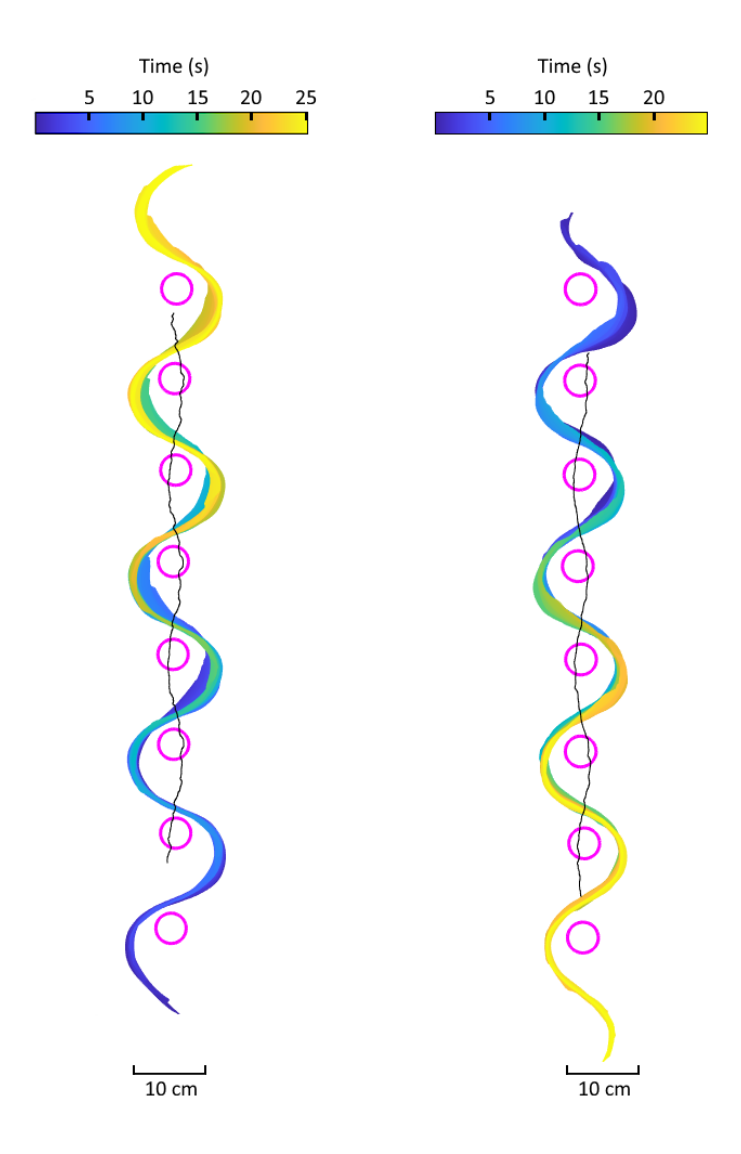


Figure 3.2: Trajectory plots for the 12.7 cm peg spacing. Movement is upwards and downwards respectively. Each plot is created from one trial, and serves as an example for the movement seen in each movement direction.

#### 3.2 Angle Between Segments

In order to better understand how well our robot snake was following the serpenoid curve it was programmed to move under, we plotted the theoretical angle between each motor based on the serpenoid equation. An example of the results of this can be seen in Fig 3.3. The angle between two vectors,  $\theta$ , can be calculated by subtracting the angle of the first vector from the second vector. Since  $\theta$  can be found by the 2 argument arctangent function, which is defined by:

$$arctan(y/x) \qquad x > 0,$$
 
$$arctan(y/x) + \pi \quad x < 0 \text{ and } y \ge 0,$$
 
$$arctan(y/x) - \pi \quad x < 0 \text{ and } y < 0,$$
 
$$\frac{\pi}{2} \qquad x = 0 \text{ and } y > 0,$$
 
$$-\frac{\pi}{2} \qquad x = 0 \text{ and } y < 0,$$
 
$$undefined \qquad x = 0 \text{ and } y = 0.$$

Since  $\theta = atan2(y, x) = arctan(y/x)$  for x>0, it follows that:

$$\theta = \phi_{i+1} - \phi_{i}$$

$$= atan2(y_{i+1}, x_{i+1}) - atan2(y_{i}, x_{i})$$

$$= atan(y_{i+1}/x_{i+1}) - atan(y_{i}/x_{i})$$

$$= atan(\frac{y_{i+1}/x_{i+1} - y_{i}/x_{i}}{1 + y_{i}y_{i+1}/x_{i}x_{i+1}})$$
Difference of arctan
$$= atan(\frac{x_{i}y_{i+1} - y_{i}x_{i+1}}{x_{i}x_{i+1} + y_{i}y_{1+1}})$$

$$= atan2(x_{i}y_{i+1} - y_{i}x_{i+1}, x_{i}x_{i+1} + y_{i}y_{i+1}),$$

where similar derivations can be performed for other values of x and y and an example of how  $\phi_i$  is defined can be seen in Fig 2.3. Following this we calculated the angle between each motor,  $\theta$ , with the equation:

$$\theta_i(t) = atan2(x_i y_{i+1} - y_i x_{i+1}, x_i x_{i+1} + y_i y_{i+1}), \tag{3.1}$$

where  $(x_i, y_i)$  is the position of the *i*th motor. An example of the results of this can be seen in Fig 3.4, which shows the angle in radians between a given body segment and the segment ahead of it as the waveform of the snake progresses through time. Due to this equation requiring two points per calculation, no angle can be computed for the first and last segment of the robot snake. Due to this, the first and last segment of the snake are also omitted from the theoretical calculation for easier comparison.

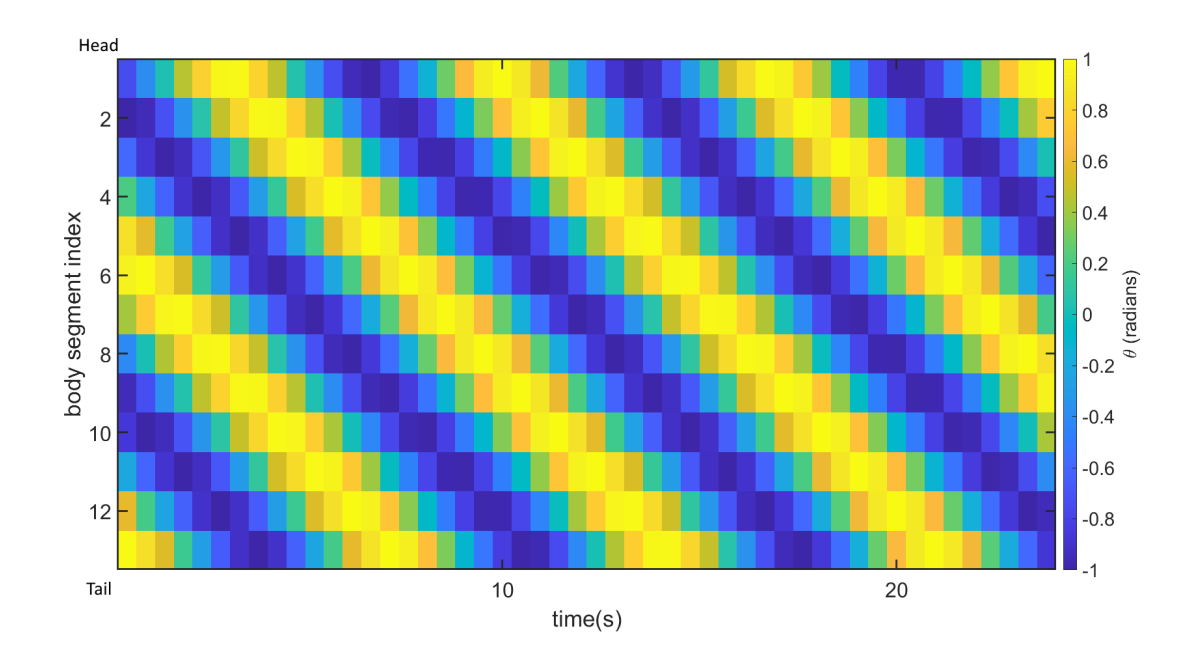


Figure 3.3: Theoretical angle between motors of a serpenoid curve corresponding to the 12.7 cm peg spacing moving upwards with respect to time.

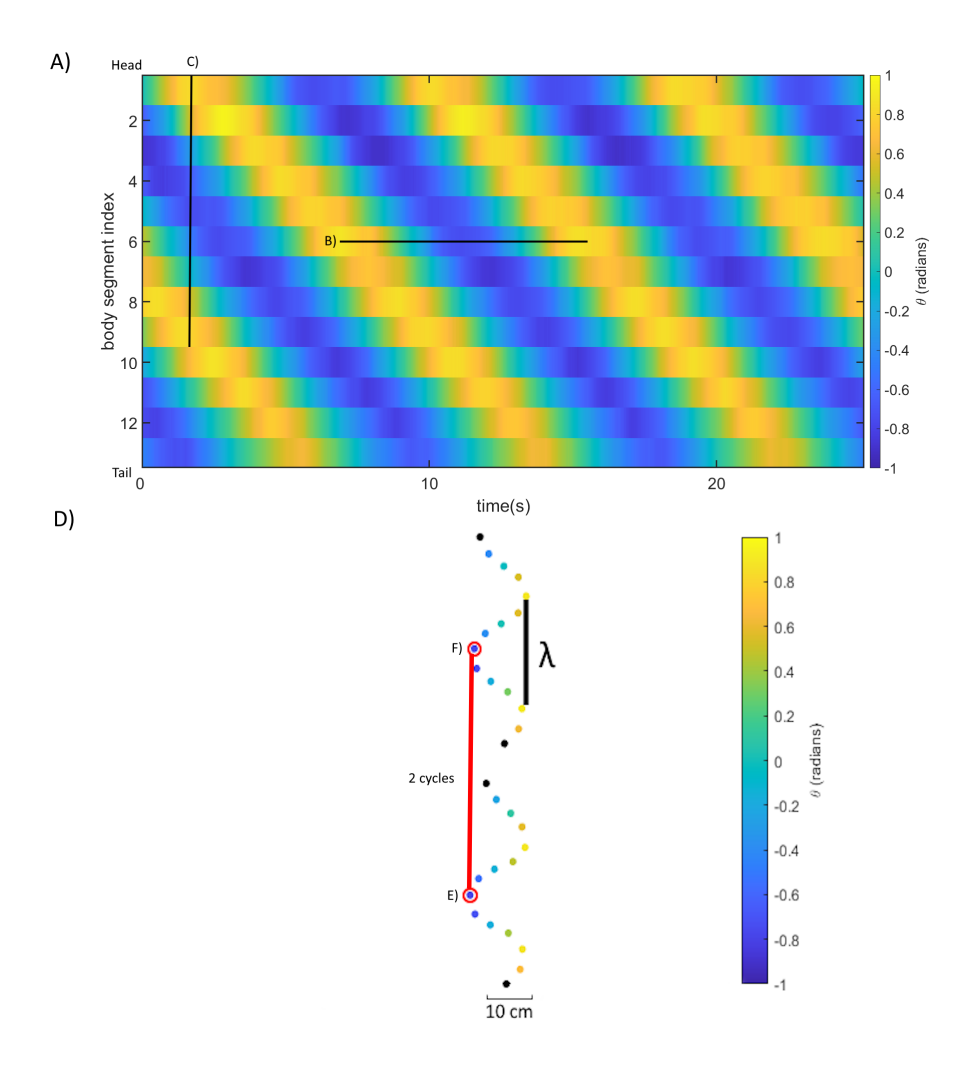


Figure 3.4: A) Measured angles between motors of a serpenoid curve corresponding to the 12.7 cm peg spacing moving upwards with respect to time. B) Horizontal line between two points in time in which a given segment has the gone through a full cycle, used to measure period. C) Vertical line between two segments with equal angles, used to measure wavelength. D) Robot snake tracking data of two different time points two cycles apart. Black points represent end of body segments that do not have an angle associated with them.  $\lambda$  is wavelength. E) A point on the robot snake's body. F) The same point two cycles later.

#### 3.3 Wavelength

Wavelength of the robot snake was calculated by finding two segments on the robot snake's body that shared the same angle at a given time step without a segment between them sharing the same angle and taking the vertical distance between these two segments. An example of how this is measured can be seen in Fig 3.4 D.



Figure 3.5: Wavelength of motion for each peg spacing, up and down. Error bars represent one standard deviation for the ten trials used to find the wavelength for a given set of parameters.

#### 3.4 Displacement Per Cycle

Center of mass velocities were calculated by analyzing each trial independently. It is assumed that the mass of the snake at each marker is approximately equal for all markers. For a given trial, the vertical and horizontal position of each marker were averaged for every time step to produce a representation of the robot snake's center of mass. Then, for every time step of a given trial other than the first time step, the previous position of the center of mass of the snake was subtracted from the current position of the center of mass of the snake, resulting in a displacement vector for the center of mass of the snake. The length of this displacement vector was then divided by the amount of time for each time step,  $\frac{1}{60}$  s, in order to find the speed of the center of mass of the snake between every frame of captured video. These speeds were then averaged to produce an average center of mass speed, which is either upwards for trials of upwards climbing or downwards for trials of downwards climbing. The average center of mass velocities for the ten trials for each set of parameters were then averaged to find an average center of mass velocity for a given set of parameters.

The time the robot snake to complete one cycle of its serpenoid wave was measured by taking the time between two maximum measures of the angle of the second segment in the snake's body, which is the segment attached to the head segment. This is assumed to represent an entire cycle for the robot snake. An example of two points separated by two cycles can be seen in Fig 3.4 E and F. An example of measuring the time to complete a cycle for a given body segment can be seen in Fig 3.4 B. The center of mass velocity was then multiplied by the time it took for the robot snake to complete one full cycle, resulting in the average displacement per cycle.

Overall the average displacement per cycle of the robot snake increased as peg spacing increased. There was a slight but noticeable decrease in average displacement per cycle for a given peg spacing when the robot snake was traveling downwards. Average displacements per cycle for each peg spacing can be seen in Fig 3.6.



Figure 3.6: Average displacement per cycle for each peg spacing, up and down. Error bars represent one standard deviation for the ten trials used to find the average displacement per cycle for a given set of parameters.

# Chapter 4

## Discussion

#### 4.1 Climbing Success

During the creation and testing of our snake robot, it was initially expected that it would be unable to climb due to its simplicity, preventing it from fully capturing the movements required for a snake to climb between pegs using lateral undulation. However, this was not what was observed. Instead, the robot snake was able to successfully climb the 12.7 cm peg spacing, and upon further testing, was able to climb the 10.2 cm and 15.2 cm peg spacings as well. Due to the smooth surface of the skin used on the robot snake, friction between the snake's body and the surface of the pegs was relatively low, suggesting that the most

important factor for a snake to be able to climb between pegs is the ability of the snake to push off of the top sides of the pegs. Therefore, it seems likely that the normal force is the most important force for determining whether or not a snake is capable of climbing between pegs, with the friction force between the snake and the pegs being less important or negligible. While our current pegboard setup does not allow for the measurement of normal forces or frictional forces, the computational model for snake climbing currently being developed by other students in the Rieser Lab will hopefully provide more insight into the relevance of friction forces for snake climbing.

#### 4.2 Trajectories

The most notable feature present in the trajectory data is the existence of areas in which the robot snake's body did not always follow the exact path that the head took on previous timesteps. These moments show up as thick sections in the trajectory data, usually right below a peg. An example of this behavior can be seen in Fig 3.1 D. This inconsistency in trajectory was likely caused due to the waveform of the snake not perfectly matching the optimal waveform for climbing the geometry of a given peg spacing, resulting in the head

of the snake attempting to rest on the next peg slightly before it had cleared the next peg, which would then cause the head of the snake to be pushed by the pegs surface to move around the peg following the correct waveform.

#### 4.3 Angle Between Segments

A notable feature of the measured angle between segments is the lower average maximum and minimum curvatures of the measured angles compared to what should be observed based on the theoretical model of the snake's motion. This can be seen when comparing Fig 3.3 to Fig 3.4, where the theoretical maximum angle between body segments should be  $\pm 1$  radian, while the observed maximum angle between body segments typically lies between  $\pm 0.7$  radians and  $\pm 0.9$  radians. While there are many possible reasons for this occurring, one of the most likely culprits is the method in which markers were attached to the snake's body. The measured angle between segments was not calculated directly from the positions of the motors, and was instead calculated based on the marker position. These markers were directly positioned above the snake's motors while the snake had no bends in its body, but as soon as the snake's body began to move, the markers would shift with the skin, no longer being directly above each motor. Therefore, directly comparing the theoretical angle

between the snake's motors to the measured angles between the snake's motors will require a more sophisticated method for the placement of markers to ensure they are no longer shifting with the snake's skin.

#### 4.4 Displacement Per Cycle

Fig 3.6 shows that the average displacement per cycle increased as the spacing between pegs increased, which is to be expected as the wavelength of the robot snake's motion also increased as the peg spacing increased, which can be seen in Fig 3.5, and we assume that the robot snake does not slip, and thus moves approximately one wavelength every cycle. Fig 3.6 also shows that average displacement per cycle decreases while traveling downwards as compared to upwards, which is also to be expected as downward movement required a slightly larger number of waves to be present on the snake's body to as the robot snake's body rests differently on the pegs during downwards motion, which can be seen in Fig 4.1, but does not match the trend expected when analyzing the wavelength of the robot snake's motion. The requirement to increase the number of waves on the robot snake's body is caused by the manner in which the robot snake rests on the pegs during climbing, where during upwards motion the side of the snake opposite the motion of travel rests on the pegs,

while during the downward trial the side of the snake that faces the same direction as the motion of travel rests on the peg. While both of these results are expected for the conditions in which the robot snake operates, real snakes are not guaranteed to follow the same trends of increasing displacement per cycle with increasing peg spacing and decreasing displacement while traveling downwards, as real snakes require time to process information gathered by their senses before moving between pegs. This has the possibility of slowing down movement between pegs spaced further apart due to the increased difficulty of reaching the next peg without slipping off the pegboard, whereas the robot snake moves with a fixed waveform that requires no additional thought.

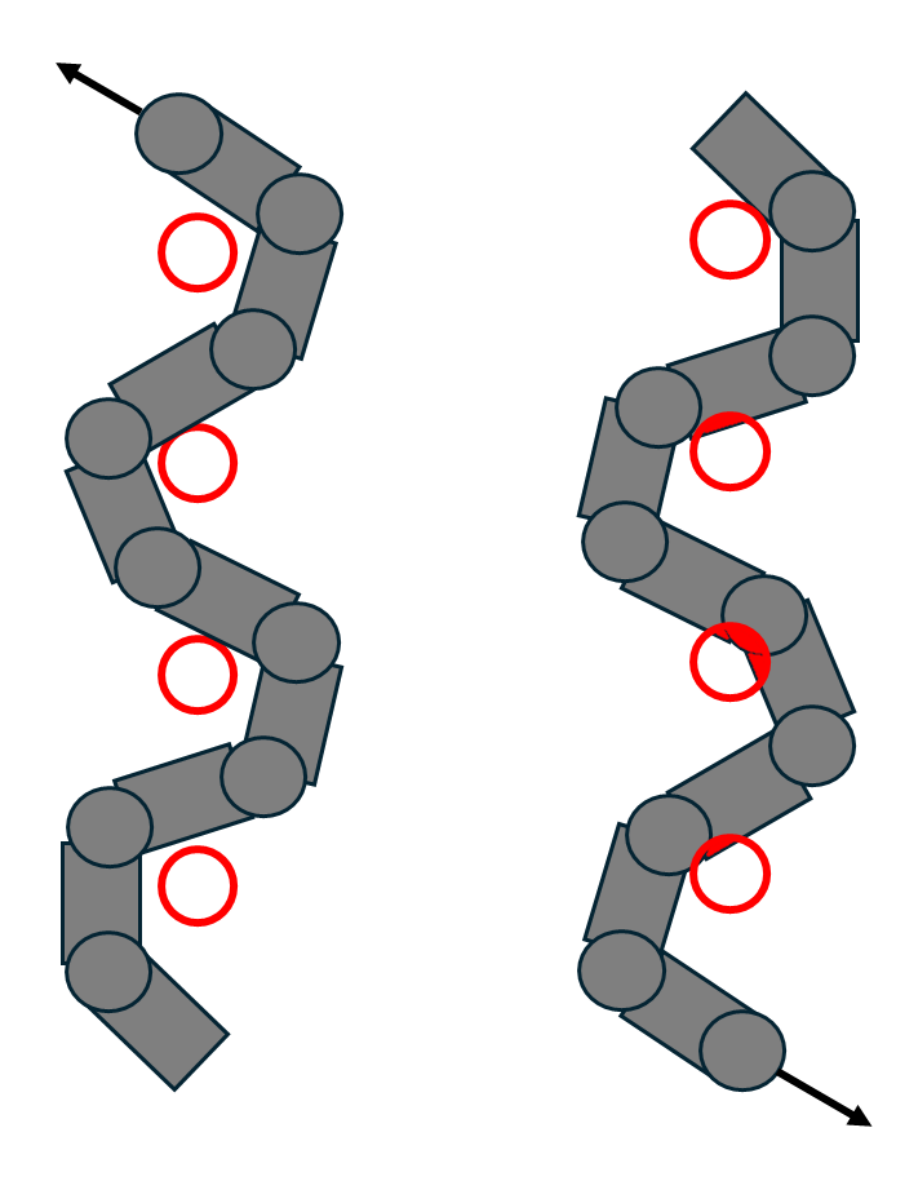


Figure 4.1: Example of robot shape that works while the robot snake is traveling upwards, but would not be possible while the robot snake is traveling downwards, resulting in the need for a slightly different set of parameters for upwards and downwards motion. Red circles represent pegs, and red areas on motors represent areas the motor could not physically occupy. Black arrows represent direction of travel.

#### 4.5 Peg Spacing Limitations

In order to climb the 10.2 cm peg spacing, the robot snake required the time between commands sent to the motors to be increased. This was due to larger amount of waves on the snake's body necessary to weave between the pegs at this short of a peg spacing, which resulted in a higher frequency waveform that caused sharper bends in the snake's body. The motors that comprise the robot snake were unable to rotate fast enough to maintain these sharp bends while being sent movement commands at the same rate as was possible with less waves on the snake's body. While lowering the rate at which commands are sent to the snake's motors allowed for the robot snake to maintain the sharp bends necessary to climb the 10.2 cm peg spacing, this reduction in command rate also came with drawbacks. Lowering the rate at which commands are sent to the motors caused the motion of the snake to become less smooth, and the motion of the snake appeared noticeably jerky. This jerkiness in the snake's motion resulted in more frequent instances of the robot snake being unable to climb the pegboard, mostly due to the snake's body jamming itself on or between the pegs, causing the motors to de-power themselves as a safety measure. While it was possible for the robot snake to climb a 10.2 cm peg spacing reliably enough to collect the data presented in this research, further exploration of movement parameters is needed to improve the smoothness of the motion of the robot snake in this regime.

It should also be noted that even though peg spacings smaller than 10.2 cm are possible, there is still a limit on how close pegs could be spaced together. At minimum this limit is equal to the width of a motor (2 cm), but in reality is larger, and is determined by the finite nature of the robot snake's body and the physical constraints applied by the width of both the robot snake's motors and the pegs the robot snake is climbing through. An example of this type of limitation can be seen in Fig 4.2.

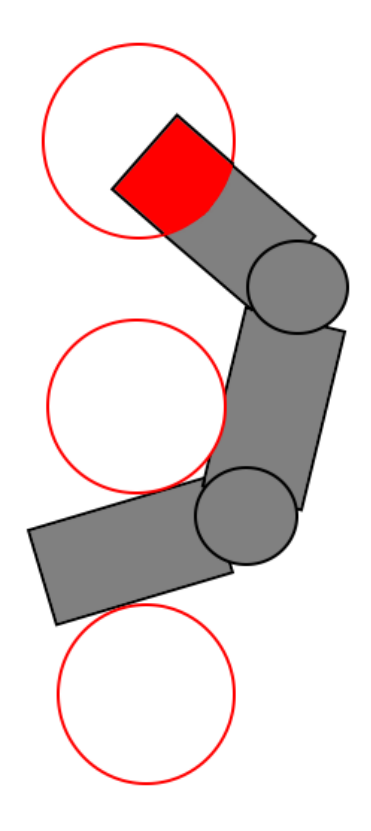


Figure 4.2: Theoretical peg spacing that would be impossible to navigate based on the physical constraints of the robot snake's body. Red circles represent pegs, and red areas on motors represent areas the motor could not physically occupy.

Trials were also conducted at a 17.8 cm peg spacing, although most of these trails were unsuccessful as the increased peg spacing resulted in less points of contact along the robot snake's body. Due to the risk of damage to our robot snake, we chose to not pursue a

complete set of successful trials at a 17.8 cm peg spacing. The robot snake was occasionally able to climb this peg spacing while maintaining very few contact points, sometimes as few as 2 points of contact, which can be seen in Fig 4.3. During moments where the robot snake experienced two points of contact, the snake's body began to pivot out of the plane of the pegboard, eventually resulting in the snake falling off the pegboard. It is possible for the robot snake to climb this peg spacing, however, it would require constant pressure on the snake's body to prevent it from falling off the pegboard, or a longer snake body that would prevent instances where the snake only maintains two contact points.

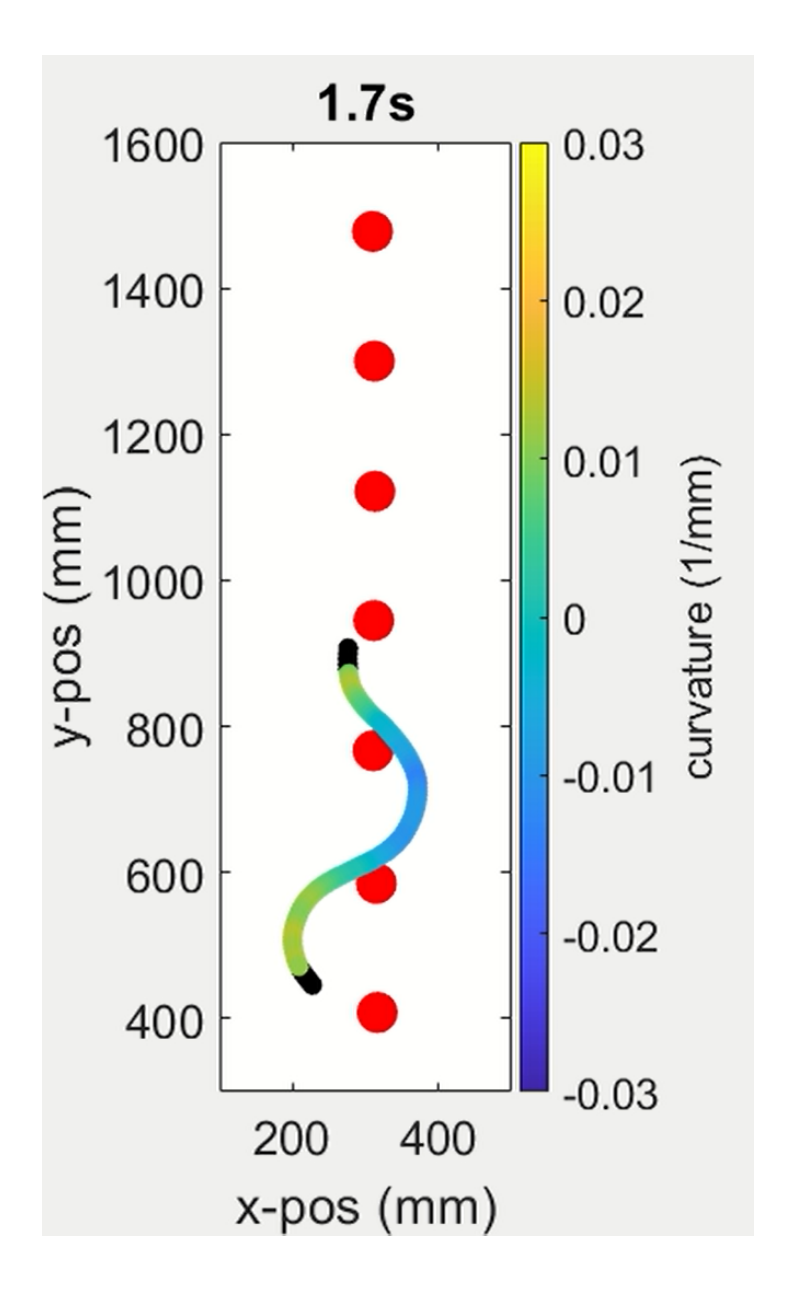


Figure 4.3: Interpolated tracking data from 17.8 cm peg spacing trial. Robot snake maintains only two points of contact at some points while climbing

# Chapter 5

## Conclusion

Through the research presented in this thesis we have accomplished the goals set forth at the beginning of our investigation. We were able to conclude that snakes are able to climb by matching the geometry of their body to the geometry of exaggerated surface features, identifying a minimal condition for snake climbing. Furthermore, we have shown that this climbing ability is not reliant on high levels of friction, and instead have shown that friction is likely not critical for this method of climbing. Lastly, we have successfully created a robot analog for snake movement that can produce consistent results under set parameters.

### 5.1 Future Work

Due to the tracking issues caused by having the markers placed directly onto the skin of the snake, we are currently investigating markers that can go through the skin of the snake and connect directly to each motor. This will allow for accurate tracking of each motor's pivot point, and will eliminate the effect of the skin being detached from the snake's body. The current iteration of this system can be seen in Fig 5.1.

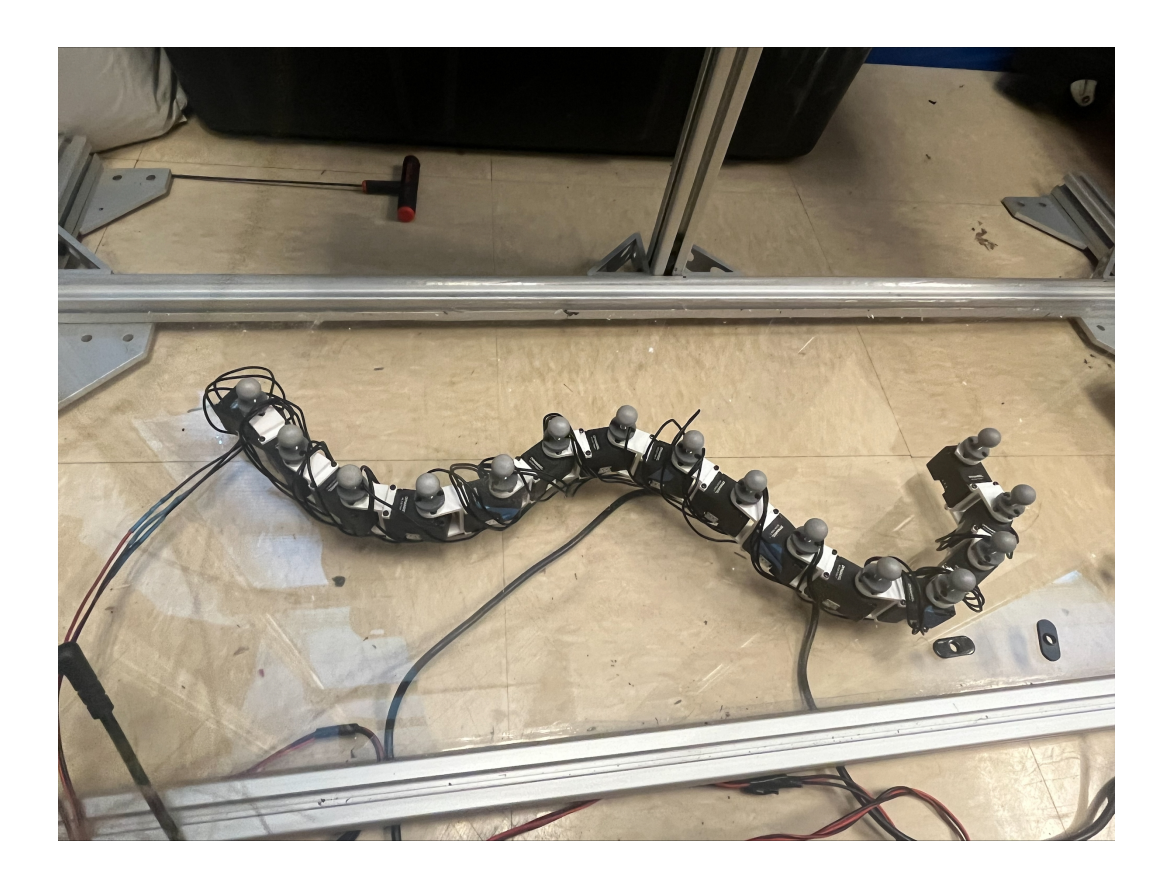


Figure 5.1: New tracking system being tested on robot snake.

We would also like to upgrade the pegboard to be force sensitive, in order to better understand how the robot snake applies force to its environment to climb the pegboard. Rieser lab currently uses a force sensitive pegboard with real snakes, however this design will need modification to be compatible with the PVC pipes used as pegs for the robot snake.

Another area we would like to investigate in the future is the ability of our robot snake to overcome disorder in its climbing environment. This could include both disorder in the pegboard, such as unevenly spaced pegs, or disorder in the robot snake's own movement inputs, such as noise being introduced to motor commands. Understanding the ability of the robot snake to overcome these difficulties will provide valuable insight into the robustness of the climbing mechanism displayed by our robot snake.

We would also like to better understand the discrepancy between the trend seen in average displacement per cycle and the trend seen in wavelength as the direction of motion was changed. The wavelength of the robot snake should decrease as the robot snake is moving downwards, as  $\xi$  is increased compared to upwards movement for the same peg spacing. However, this is not the trend that we measured in the trials we conducted, which prompts further inqury into the cause of this trend.

#### 5.2 Applications

A practical use for simple limbless robots like our robot snake is the navigation of areas that would be too dangerous for humans to enter. This could include aiding rescue attempts in collapsed buildings or other hard to enter areas through the use of an attached camera, or carrying items through small spaces that would otherwise be difficult to navigate. This has already been achieved by other groups [26], whose robot can be seen in Fig 1.4 A, though their robots typically focused on climbing by wrapping around a pole and climbing using concertina locomotion. While our snake robot has only been used to climb regularly spaced pegs at this point, in the future we hope that the knowledge gained from these experiments will inform more complex robots that can traverse diverse environments, including areas with protrusions similar to branches or pegs.

# Bibliography

- Moon, B., Gans, C. "Kinematics, Muscular Activity and Propulsion in Gopher Snakes".
   J Exp Biol. 201 (19): 2669–2684. doi:https://doi.org/10.1242/jeb.201.19.2669
- [2] Gray, J., Lissmann, H. "The Kinetics of Locomotion of the Grass-Snake". (1950). J Exp Biol 26 (4): 354–367. doi: https://doi.org/10.1242/jeb.26.4.354
- [3] Marvi, H., Cook, J., Streator, J., Hu, D. "Snakes move their scales to increase friction", (2016). Biotribology, Volume 5, Pages 52-60, ISSN 2352-5738, https://doi.org/10.1016/j.biotri.2015.11.001.
- [4] Gray, J. "The Mechanism of Locomotion in Snakes". (1946). J Exp Biol 23 (2): 101–120. doi: https://doi-org.proxy.library.emory.edu/10.1242/jeb.23.2.101

- [5] Carl, G. "How Snakes Move." (1970). Scientific American, vol. 222, no. 6, pp. 82–99.
   JSTOR, http://www.jstor.org/stable/24925828.
- [6] Ma, S. "Analysis of snake movement forms for realization of snake-like robots," (1999). Proceedings 1999 IEEE International Conference on Robotics and Automation (Cat. No.99CH36288C), Detroit, MI, USA, pp. 3007-3013 vol.4, doi: 10.1109/ROBOT.1999.774054.
- [7] Harvey Lillywhite. 2014. How Snakes Work. Oxford University Press, Inc., USA. ISBN: 9780195380378.
- [8] Harry Greene, Michael Fogden, Patricia Fogden. 2000. Snakes: The Evolution of Mystery in Nature. University of California Press, USA.
- [9] Emma Huddleston. 2020. How Snakes Slither (The Science of Animal Movement). Abdo Group, Minneapolis, MN, USA.
- [10] Pål Liljebäck, K.Y. Pettersen, Øyvind Stavdahl, Jan Gravdahl. (2013). Snake Robots: Modelling, Mechatronics, and Control. 10.1007/978-1-4471-2996-7.
- [11] Cowles, R. B. "Sidewinding Locomotion in Snakes". (1956). Copeia, 1956(4), 211–214. https://doi.org/10.2307/1440272

- [12] Harrington, S., de Haan, J., Shapiro, L., Ruane, S. "Habits and characteristics of arboreal snakes worldwide: arboreality constrains body size but does not affect lineage diversification", (2018). Biological Journal of the Linnean Society, Volume 125, Issue 1, September 2018, Pages 61–71, https://doi.org/10.1093/biolinnean/bly097
- [13] Jayne, B. "What Defines Different Modes of Snake Locomotion?", (2020).
  Integrative and Comparative Biology, Volume 60, Issue 1, Pages 156–170, https://doi.org/10.1093/icb/icaa017
- [14] Marvi, H., et al. "Sidewinding with minimal slip: Snake and robot ascent of sandy slopes".(2014). Science 346, 224-229. DOI:10.1126/science.1255718
- [15] Astley, H.C., Gong, C., Dai, J., Travers, M., Serrano, M.M., Vela, P.A., Choset, H., Mendelson, J.R., Hu, D.L., Goldman, D.I. "Modulation of orthogonal body waves enables high maneuverability in sidewinding locomotion", (2015). Proc. Natl. Acad. Sci. U.S.A. 112 (19) 6200-6205
- [16] Tingle, J. "Facultatively Sidewinding Snakes and the Origins of Locomotor Specialization", (2020). Integrative and Comparative Biology, Volume 60, Issue 1, Pages 202–214, https://doi.org/10.1093/icb/icaa011

- [17] Capano, J. "Reaction Forces and Rib Function During Locomotion in Snakes", (2020).
  Integrative and Comparative Biology, Volume 60, Issue 1, July 2020, Pages 215–231, <a href="https://doi.org/10.1093/icb/icaa033">https://doi.org/10.1093/icb/icaa033</a>
- [18] Seyidoğlu, B., Rafsanjani, A. "A textile origami snake robot for rectilinear locomotion", (2024). Device. Volume 2, Issue 2. 100226
- [19] Marvi, H., Hu, D. "Friction enhancement in concertina locomotion of snakes". (2012).
  J. R. Soc. Interface, doi:10.1098/rsif.2012.0132
- [20] Byrnes, G., Jayne B.C. "Gripping during climbing of arboreal snakes may be safe but not economical". (2014). Biol. Lett. 10: 20140434. http://dx.doi.org/10.1098/rsbl.2014.0434
- [21] Jurestovsky, D., Usher, L., Astley, H. "Generation of propulsive force via vertical undulations in snakes". (2021). J Exp Biol 1 July 2021; 224 (13): jeb239020. doi: https://doi.org/10.1242/jeb.239020
- [22] Saranli, U., Buehler, M., Koditschek, DE. "RHex: A Simple and Highly Mobile Hexapod Robot". (2001). The International Journal of Robotics Research. 2001;20(7):616-631. doi:10.1177/02783640122067570

- [23] Aguilarl, J., et al. "A review on locomotion robophysics: the study of movement at the intersection of robotics, soft matter and dynamical systems" (2016). Rep. Prog. Phys. 79 110001 DOI 10.1088/0034-4885/79/11/110001
- [24] Trevelyan, T. "Simplifying robotics A challenge for research", (1997). Robotics and Autonomous Systems, Volume 21, Issue 3, Pages 207-220, ISSN 0921-8890, https://doi.org/10.1016/S0921-8890(97)00075-4.
- [25] Wright, C., Buchan, A., Brown, B., Geist, J., Schwerin, M., Rollinson, D., Tesch, M., and Choset, H. "Design and architecture of the unified modular snake robot," in 2012 IEEE International Conference on Robotics and Automation (ICRA). IEEE, 2012, pp. 4347–4354.
- [26] Whitman, J., Zevallos, N., Travers, M., Choset, H. "Snake Robot Urban Search After the 2017 Mexico City Earthquake," (2018). 2018 IEEE International Symposium on Safety, Security, and Rescue Robotics (SSRR), Philadelphia, PA, USA, pp. 1-6, doi: 10.1109/SSRR.2018.8468633..
- [27] Lam, T., Xu, Y. "A flexible tree climbing robot: Treebot design and implementation," (2011) 2011 IEEE International Conference on Robotics and Automation, Shanghai, China, pp. 5849-5854, doi: 10.1109/ICRA.2011.5979833.

- [28] Takemori, T., Tanaka, M., Matsuno, F. "Ladder Climbing with a Snake Robot," (2018).
  2018 IEEE/RSJ International Conference on Intelligent Robots and Systems (IROS),
  Madrid, Spain, pp. 1-9, doi: 10.1109/IROS.2018.8594411.
- [29] Wright, C., et al., "Design of a modular snake robot," 2007 IEEE/RSJ International Conference on Intelligent Robots and Systems, San Diego, CA, USA, 2007, pp. 2609-2614, doi: 10.1109/IROS.2007.4399617.
- [30] Fu, Q., Li, C. "Robotic modelling of snake traversing large, smooth obstacles reveals stability benefits of body compliance" (2020). R. Soc. Open Sci. 7191192 http://doi.org/10.1098/rsos.191192
- [31] Marvi, H., Meyers, G., Russell, G., Hu, D. "Scalybot: A Snake-Inspired Robot With Active Control of Friction." (2011) ASME 2011 Dynamic Systems and Control Conference and Bath/ASME Symposium on Fluid Power and Motion Control, DSCC 2011. 2. 10.1115/DSCC2011-6174.
- [32] Shigeo Hirose, Peter Cave, and Charles Goulden. 1993. Biologically Inspired Robots: Serpentile Locomotors and Manipulators. Oxford University Press, Inc., USA.

[33] The MathWorks Inc. (2025). ${\rm makima}$ Modified  ${\bf Akima}$ piecewise cu- ${\rm bic}$ Hermite interpolatio, Natick, Massachusetts: The MathWorks  ${\rm Inc.}$  $https://www.mathworks.com/help/matlab/ref/makima.html\#mw\_e8ee1c8c-2cc3-makima.html\#mw\_e8ee1c8c-2cc3-makima.html$  $46\mathrm{c}4\text{-}90\mathrm{c}4\text{-}\mathrm{c}3208804\mathrm{ff}4\mathrm{el}$